Earth Syst. Sci. Data Discuss., 8, 809–825, 2015
www.earth-syst-sci-data-discuss.net/8/809/2015/
doi:10.5194/essdd-8-809-2015

Open Access Earth System Science Data Discussions

This discussion paper is/has been under review for the journal Earth System Science Data (ESSD). Please refer to the corresponding final paper in ESSD if available.

In situ measurement of the biogeochemical properties of Southern Ocean mesoscale eddies in the Southwest Indian Ocean, April 2014

S. de Villiers, K. Siswana, and K. Vena

Oceans and Coastal Research, Department of Environmental Affairs, Cape Town, South Africa

Received: 3 September 2015 – Accepted: 23 September 2015 – Published: 2 October 2015

Correspondence to: S. de Villiers (steph.devilliers@gmail.com)

Published by Copernicus Publications.

Abstract

Several open-ocean mesoscale features, a "young" warm-core (anti-cyclonic) eddy at 52° S, an "older" warm-core eddy at 57.5° S, as well as an adjacent cold-core (cyclonic) eddy at 56° S, were surveyed during a M/V *S.A. Agulhas II* cruise in April 2014. The main aim of the survey was to obtain hydrographical and biogeochemical profile data for contrasting open-ocean eddies in the Southern Ocean, that will be suitable for comparison and modelling of their heat, salt and nutrient characteristics, and the changes that occur in these properties as warm-core eddies migrate from the polar front southwards into the Southern Ocean. Results show that the older warm-core eddy at 57.5° S is, at its core, 2.7 °C colder than a younger eddy at 52° S, while its dissolved silicate levels are almost 500 % higher and accompanied by chl *a* levels that are more than 200 % higher than that in the younger eddy. A total of 18 CTD stations were occupied in a sector south of the Southwest Indian Ridge, along three transects crossing several mesoscale features identified from satellite altimetry data prior to the cruise. The CTD data, as well as chl *a* and dissolved nutrient data (for NO_3^-, NO_2^-, PO_4^{3-} and SiO_2) have been processed, quality-controlled and made available via the PANGAEA Data Archiving and Publication database at doi:10.1594/PANGAEA.848875.

1 Introduction

The circulation and thermohaline structure of the Southern Ocean is of critical importance to global exchanges of heat, freshwater and biogeochemical constituents such as nutrients and CO_2. A detailed understanding of the role of mesoscale eddy transport in these processes is still lacking. It has only fairly recently been established that mesoscale eddies contain most of the kinetic energy of ocean circulation (Fu et al., 2010; Ferrari and Wunch, 2009) and that the global eddy volume transport is comparable in magnitude to that of large-scale wind- and thermohaline-driven circulation (Zhang et al., 2014). It is now estimated that in the open ocean most of the vertical transport

ESSDD
8, 809–825, 2015

of biogeochemical properties, such as nutrients, takes place at the sub-mesoscale, associated with eddies (Klein and Lapeyre, 2009; McGillicuddy et al., 2007; Lévy et al., 2001). At the global scale, areas of enhanced eddy kinetic energy usually also exhibit elevated levels of marine primary productivity (Chelton et al., 2011; Falkowski et al., 1991; Siegel et al., 2011). However, our understanding of the global significance of large-scale coincident patterns of enhanced open ocean productivity and mesoscale activity, and the dynamics of eddy-driven nutrient pumps, is still in its infancy.

Progress in this field, including the incorporation of biogeochemical cycles into eddy-resolving GCM's, is severely limited by scarce in situ data, collected with the specific aim of improving our understanding of the physical and biogeochemical processes associated with mesoscale features such as eddies. This lack of in situ data is particularly pronounced in the Southern Ocean. Despite the significance of the Southern Ocean to ocean-atmosphere CO_2 exchange and global climate, and the important role of ocean eddies to these processes (Frenger et al., 2013; Sheen et al., 2014; Morrow et al., 1994), it remains a remote, hostile and under-sampled ocean environment.

The objective of this paper is to present an overview of in situ data that had been collected in the Southern Hemisphere autumn, across a number of important mesoscale features in the southwestern Indian Ocean sector of the Southern Ocean (Fig. 1), and to make this data set available to the scientific community. Interaction of the Antarctic Circumpolar Current with the shallow topographic features of the Southwest Indian Ocean Ridge (SWIR) play an important role in the generation of open ocean eddies just south of the polar front (Gouretski and Danilov, 1994; Pollard and Read, 2001; Durgadoo et al., 2011). The subsequent movement of these eddies in a southerly direction, into the Southern Ocean proper, represents an ideal natural laboratory for the in situ observation and study of the eddy transport of heat, salt and chemicals across strong frontal zones in the Southern Ocean. To date, detailed studies of the chemical characteristics of such eddies and the evolution of these properties over time and distance, have not been carried out. This represents an important knowledge gap, par-

ESSDD
8, 809–825, 2015

ticularly with regards to understanding Southern Ocean nutrient transport processes and carbon cycling.

2 Sampling survey design

The survey cruise was conducted from 2 April to 6 May 2014 (EXPOCODE 91AH20140402), the austral autumn, as part of the Department of Environmental Affairs' 2014 Marion Relief Voyage 011 on the M/V *S.A. Agulhas II*, to its base in the subantarctic Prince Edward Islands (Fig. 1a). The M/V *S.A. Agulhas II* is a relatively new (commissioned in 2012) polar research and supply vessel, fully equipped for ship-based oceanographic research. Facilities include a moon pool, that can be used as a CTD launch area, even in the event of severe weather conditions.

Several months prior to the ship survey, evaluation of satellite altimetry sea surface height anomaly (SSHA) data was initiated, to identify and track the position of eddies suitable for study. Composite sea-surface height anomaly (SSHA) satellite altimetry data, representing the sampling period, were obtained from the online data viewer of the Colorado Center for Astrodynamics Research (CCAR) (http://eddy.colorado.edu/ccar/data_viewer/index) (Fig. 1b). The global Historical Gridded SSH data viewer was used, which typically include ±10 days of Topex/Poseidon, Jason-a and Jason-2/OSTM data. MODIS-aqua satellite derived chlorophyll data could not be used to complement the SSHA data, due to extensive cloud cover over the study area during the survey period.

Mesoscale features with positive SSH anomalies, identified from satellite altimetry, were assumed to represent anti-cyclonic, warm-core eddies (Fig. 1b). Similarly, features with negative SSHA values were assumed to be cyclonic, cold-core eddies. Observation of the evolution of the SSHA characteristics of mesoscale features over several months suggested that larger positive SSHA values can be assumed to represent younger, more recently formed, anti-cyclonic eddies. Ship-based ADCP data (M. van den Berg, unpublished cruise report contribution) confirmed the direction

ESSDD
8, 809–825, 2015

of anti-cyclonic and cyclonic flow around the features identified as respectively anti-cyclonic and cyclonic eddies from satellite altimetry.

On the basis of satellite SSHA images (Fig. 1b), the following three main mesoscale features were identified for detailed study prior to the start of CTD transects, within the constraints of the ship-time available (with approximate eddy core positions and SSHA at time of survey, Table 1):

- a "young, warm-core" anti-cyclonic eddy, at 52° S, 30.2° E (core SSHA $>$ 40 cm)
- a "mature, warm-core" anti-cyclonic eddy, at 57.5° S, 29.5° E (core SSHA $>$ 20 cm)
- a "cold-core" cyclonic eddy feature, at 56° S, 29.5° E (core SSHA < -20 cm)

Based on the identification of these three mesoscale features, the following three transects (E1 to E3 in Fig. 1b) were decided on for detailed CTD profiling (station locations in Table 1) and water column sampling for chemical analysis:

- *Transect E1* (15 to 16 April 2014): North-to-South transect from 55 to 58.5° S, along 29.5° E; 8 CTD stations were occupied at 0.5° latitude intervals; the main features along this transect were the "mature" warm-core eddy and a cold-core cyclonic eddy just north of it;
- *Transect E2* (17 to 19 April 2014): East-to-West transect from 32 to 28.25° E, along 57.5° S; 6 CTD stations were occupied along this transect, at 0.75° longitude intervals; the main feature along this transect is the mature warm-core eddy;
- *Transect E3* (21 to 22 April 2014): West-to-East transect along 52° S, from 28.3 to 31° E; 4 CTD stations were occupied along this transect, at approximately 0.75° longitude intervals; the main feature along this transect was the relatively young, warm-core eddy.

ESSDD
8, 809–825, 2015

3 Seawater sampling and analysis

Two SBE 9plus CTD systems, a moon pool CTD with a 24 20-L Niskin bottle rosette, or alternatively a 12 10-L Niskin bottle rosette for over-the-side deployment, were used for water column profiling and discrete water sampling at standard depths. The CTD deployments along the most southerly transects (E1 and E2), had to be conducted with the moon pool CTD, as a result of the extremely high seas and inclement weather during the survey period, which ruled out over-the-side deployment of equipment. The moon pool CTD was lost after completion of transects E1 and E2, as a result of damage sustained in very rough seas, and transect E3 was carried out with the smaller CTD. Water temperature was measured to a precision of ±0.0001 °C. Salinity was computed from CTD data in practical salinity units (PSU) and calibrated using discrete samples (precision ±0.0001 PSU). The CTD oxygen sensor was calibrated with oxygen measurements obtained from discrete samples at selected depths, applying the Winkler titration method using an electronic stand (Hansen, 1999). The precision of the oxygen titration was ±0.45 $\mu mol\,kg^{-1}$. Turbidity, given in Nepholometric Turbidity Units (NTU), was measured using the original calibration provided by the company.

Seawater samples for chemical analysis were collected from the Niskin bottles, at standard depths. Samples for dissolved oxygen analysis were collected from the Niskin bottles via silicone tubing, taking care not to introduce or trap air bubbles. For dissolved inorganic nutrient analysis, acid-washed 15 mL polypropylene tubes were thoroughly rinsed with sample water before filling and frozen at −80 °C prior to ship-based analysis using an Astoria AutoAnalyser Series 300, expanded to four channels. Dissolved nitrate (NO_3^-), nitrite (NO_2^-) and silicate (SiO_2) were determined following the methods of Armstrong et al. (1967) and phosphate (PO_4^{3-}) according to the methods of Bernhardt and Wilhelms (1967).

Samples for chl *a* analysis were taken at four depths (near-surface, above the fluorescence maximum (F-max), F-max and below the F-max). Sub-samples (200 mL) of seawater for chl *a* analysis were collected in pre-rinsed plastic bottles. Samples were

ESSDD
8, 809–825, 2015

immediately filtered, under vacuum onto 25 mm Whatman™ GF/F glass fibre filter papers (Parsons et al., 1984). The filter papers were frozen in aluminium foil pouches prior to analysis. Chl *a* was measured fluorometrically on a Turner Designs 10-AU fluorometer after extraction in 90 % acetone (Welschmeyer, 1995). The fluorometer was calibrated with chl *a* standard (Sigma Chemical Co., USA) in 90 % acetone solution with a GBC Cintra 404 spectrophotometer and an extraction coefficient of 87.67 $\mathrm{L\,g^{-1}\,cm^{-1}}$.

4 Data overview and discussion

In situ CTD profiling data confirmed the presence and position of the anti-cyclonic and cyclonic eddies, targeted for study based on SSHA observational data (Figs. 2a–c and 3). The mature, warm (or anti-cyclonic) eddy at 57.5° S (Table 1) has a maximum core temperature of 2.2 to 2.35 °C, which is observed in the 200 to 300 m depth range (Fig. 3). In a 150 m deep upper mixed layer, water in this eddy core has been cooled down to ∼ 1.95 °C, presumably through heat exchange with the overlaying atmosphere and surrounding water masses. In the core of the cold-core eddy located 1.5° north of this, temperature reaches maximum values of almost 1.85 °C, which is observed in the upper 100 m of the water column. The young, warm-core eddy much further north at 52° S, in contrast, is characterised by core temperatures of around 4.7 °C in the well-mixed upper 100 m layer, and around 3 to 2.6 °C in the 200 to 300 m depth range. The sampling survey, therefore, successfully captured the very different temperature characteristics, and heat content, of eddies with contrasting origins and histories. The in situ capturing of such differences provides meaningful data for the quantification and modelling of heat exchange processes related to eddy movement in the Southern Ocean.

The average value of physical and chemical parameters for the upper 100 m of the water column is summarized for all CTD stations in Table 2 and profile data for salinity, nutrients an chl *a* shown in Fig. 2d–f, Figs. 4 and 5. The data demonstrate a number of significance differences between the eddies:

ESSDD
8, 809–825, 2015

– in the upper 100 m, the young warm-core eddy (E3-3) is 2.74 °C warmer, slightly less saline, with silicate levels almost a fifth, and chl *a* levels more than a factor of 2 lower, than that in its older equivalent further south (E1-6)

The upper ocean water property characteristics of the adjacent cold and mature warm eddies, at 56 and 57.5° S respectively, are much more similar to each other than is the case for the younger versus older warm-core eddies (Table 2). The cold eddy is, on average, only 0.13 °C colder, with approximately the same upper ocean salinity values. The old warm-core eddy has slightly higher upper ocean phosphate and nitrate concentrations than the cold eddy, 6 and 5 % respectively, but significantly higher chl *a* (+63 %) and lower silicate levels (−17 %).

The data show that there are pronounced changes in surface ocean dissolved silicate and chl *a* characteristics of warm-core eddies as they migrate from the polar front, southwards into the Southern Ocean. Increasing levels of silicate in warm-core eddies are presumably the result of lateral and/or vertical mixing with adjacent silicate-rich water masses. This results in dramatically increased levels of productivity. Bongo net tows conducted during the survey (unpublished results), confirmed that the increased levels of chl *a*, south of the polar front, are associated with diatom productivity. The nutrient and chl *a* profile data presented here provide valuable input data for the modelling of the complex biogeochemical processes associated with mesoscale activity in the Southern Ocean.

Author contributions. S. de Villiers determined the sampling strategy, collected samples, and oversaw and collated the measurements; K. Siswana and K. Vena assisted in sample collection, chemical analysis and data presentation; S. de Villiers prepared the manuscript.

Acknowledgements. All ship-based participants, crew and research staff, in some way or another contributed to the collection of this dataset, and their contributions are gratefully acknowledged. The Chief Scientist for the cruise was H. Verheye, and the cruise and associated research activities were financed by the Department of Environmental Affairs.

References

Armstrong, F. A. J., Stearns, C. A., and Strickland, J. D. H.: The measurement of upwelling and subsequent biological processes by means of the Technicon Autoanalyzer and associated equipment, Deep-Sea Res., 14, 381–389, 1967.

Bernhardt, H. and Wilhelms, A.: The continuous determination of low level iron, soluble phosphate and total phosphate with the AutoAnalyzer, Technicon Symposia I, 385–389, 1967.

Chelton, D. B., Gaube, P., Schlax, M. G., Early, J. J., and Samelson, R. M.: The influence of nonlinear mesoscale eddies on near-surface oceanic chlorophyll, Science, 334, 328–332, 2011.

Dong, S., Sprintall, J., and Gille, S. T.: Location of the Antarctic Polar Front from AMSR-E satellite sea surface temperature measurements, J. Phys. Ocean., 36, 2075–2089, 2006.

Durgadoo, J. V., Ansorge, I. J., de Cuevas, B. A., Lutjeharms, J. R. E., and Coward, A. C.: Decay of eddies at the South-West Indian Ridge, S. Afr. J. Sci., 107, 673, doi:10.4102/sajs.v107i11/12.673, 2011.

Falkowski, P., Ziemann, D., Kolber, Z., and Bienfang, P.: Role of eddy pumping in enhancing primary production in the ocean, Nature, 352, 55–58, 1991.

Ferrari, R. and Wunch, C.: Ocean circulation kinetic energy: reservoirs, sources, and sinks, Annu. Rev. Fluid Mech., 41, 253–282, 2009.

Frenger, I., Gruber, N., Knutti, R., and Münnich, M.: Imprint of Southern Ocean eddies on winds, clouds and rainfall, Nat. Geosci., 6, 608–612, 2013.

Fu, L.-L., Chelton, D. B., Le, P.-Y., and Morrow, R.: Eddy dynamics from satellite altimetry, Oceanography, 23, 14–25, 2010.

Gouretski, V. V. and Danilov, A. I.: Characteristic of warm rings in the African sector of the Antarctic Circumpolar current, Deep-Sea Res., 41, 1131–1157, 1994.

Hansen, H. P.: Determination of oxygen, in: Methods of Seawater analysis, edited by: Grasshoff, K. K. and Ehrhardt M., Wiley-VCH, Weinheim, 75–89, 1999.

Klein, P. and Lapeyre, G.: The oceanic vertical pump induced by mesoscale and submesoscale turbulence, Annu. Rev. Mar. Sci., 1, 351–375, 2009.

Lévy, M., Klein, P., and Treguier, A.-M.: Impact of sub-mesoscale physics on production and subduction of phytoplankton in an oligotrophic regime, J. Mar. Res., 59, 535–565, 2001.

McGillicuddy Jr., D. J., Anderson, L. A., Bates, N. R., Bibby, T., Buesseler, K. O., Carlson, C. A., Davis, C. S., Ewart, C., Falkowski, P. G., Goldthwait, S. A., Hansell, D. A., Jenkins, W.

ESSDD
8, 809–825, 2015

J., Johnson, R., Kosnyrev, V. K., Ledwell, J. R., Li, Q. P., Siegel, D. A., and Steinberg, D. K.: Eddy/wind interactions stimulate extraordinary mid-ocean plankton blooms, Science, 316, 1021–1026, 2007.

Morrow, R. A., Coleman, R., Church, J. A., and Chelton, D. B.: Surface eddy momentum flux and velocity variance in the Southern Ocean from GEOSAT altimetry, J. Phys. Ocean., 24, 2050–2071, 1994.

Parsons, T. R., Maita, Y., and Lalli, C. M.: A Manual of Chemical and Biological Methods for Seawater Analysis, Pergamon Press, Oxford, 173 pp., 1984.

Pollard, R. T. and Read, J. F.: Circulation pathways and transports of the Southern Ocean in the vicinity of the Southwest Indian Ridge, J. Geophys Res., 106, 2881–2898, doi:10.1029/2000JC900090, 2001.

Sheen, K. L., Garabato, A. C. N., Brearley, J. A., Meredith, M. P., Polzin, K. L., Smeed, D. A., Forryan, A., King, B. A., Sallée, J.-B., St. Laurent, L., Thurnherr, A. M., Toole, J. M., Waterman, S. N., and Watson, A. J.: Eddy-induced variability in Southern Ocean abyssal mixing on climatic timescales, Nat. Geosci., 7, 577–582, 2014.

Siegel, D., Peterson, P., McGillicuddy, D., Maritorena, S., and Nelson, N.: Bio-optical footprints created by mesoscale eddies in the Sargasso Sea, Geophys. Res. Lett., 38, L13608, doi:10.1029/2011GL047660, 2011.

Welschmeyer, N. A. and Waterhouse, T. Y.: Taxon-specific analysis of microzooplankton grazing rates and phytoplankton growth rates, Limnol. Oceanogr., 40, 827–834, 1995.

Zhang, Z., Wang, W., and Qui, B.: Oceanic mass transport by mesoscale eddies, Science, 345, 322–324, 2014.

ESSDD

8, 809–825, 2015

ESSDD
8, 809–825, 2015

In situ measurement of the biogeochemical properties

S. de Villiers et al

Table 1. CTD station locations and identification of CTD station positions relative to eddy cores, as inferred from altimetry data. E1, E2 and E3 refer to the three transect lines shown in Fig. 1. E1-6 is a mature warm-core eddy, and E3-3 a younger warm-core eddy, based on interpretation of relative SSH anomalies associated with these two eddies.

Ship Station	ID	Position relative to eddy core	Sampling Date	Latitude (° S)	Longitude (° E)	Depth (m)
AM00264	E1-1	1° N of cold-core	15 April 2014	54.99967	29.50067	4506
AM00265	E1-2	0.5° N of cold-core	15 April 2014	55.49967	29.50083	5296
AM00266	E1-3	Cold-core	15 April 2014	55.99967	29.50100	5581
AM00267	E1-4	0.5° S of cold-core	15 April 2014	56.50100	29.50617	5288
AM00268	E1-5	0.5° N of warm-core	16 April 2014	57.00067	29.50100	5275
AM00269	E1-6	Warm-core	16 April 2014	57.50033	29.50233	5565
AM00270	E1-7	0.5° S of warm-core	16 April 2014	57.99950	29.50050	5261
AM00271	E1-8	1° S of warm-core	16 April 2014	58.50100	29.50183	5534
AM00272	E2-1	2.5° E of warm-core	17 April 2014	57.48300	32.00133	5550
AM00273	E2-2	1.75° E of warm-core	18 April 2014	57.50017	31.25083	5262
AM00274	E2-3	1° E of warm-core	18 April 2014	57.50050	30.50233	5270
AM00275	E2-4	0.25° E of warm-core	18 April 2014	57.50000	29.75183	5269
AM00276	E2-5	0.5° W of warm-core	19 April 2014	57.49983	29.00067	5268
AM00277	E2-6	1.25° W of warm-core	19 April 2014	57.50050	28.25117	5135
AM00281	E3-1	1.9° W of warm-core	21 April 2014	52.00017	28.33500	5481
AM00282	E3-2	0.73° W of warm-core	22 April 2014	52.00700	29.50100	5379
AM00283	E3-3	Warm-core	22 April 2014	52.00933	30.22617	3817
AM00284	E3-4	0.78° E of warm-core	22 April 2014	51.99900	31.00233	5154

Table 2. Average upper ocean (surface to 100 m) physical and chemical water column characteristics, obtained from CTD profiles, in and around warm and cold eddies. Samples for nutrient and chlorophyll *a* analysis were not collected at CTD stations E2-1 and E3-1.

ID	Position relative to eddy core	T (°C)	S (psu)	SiO_2 (µmol kg^{-1})	PO_4^{3-} (µmol kg^{-1})	NO_3^- (µmol kg^{-1})	Chl *a* (µg L^{-1})
E1-1	1° N of cold-core	2.31	33.97	29.9	1.50	20.9	0.14
E1-2	0.5° N of cold-core	1.75	33.98	29.6	1.37	20.4	0.33
E1-3	Cold-core	1.83	33.98	30.8	1.47	21.6	0.35
E1-4	0.5° S of cold-core	1.99	33.95	29.3	1.58	23.6	0.36
E1-5	0.5° N of warm-core	1.77	33.96	27.6	1.53	22.7	0.58
E1-6	Warm-core	1.96	33.98	25.7	1.56	22.7	0.57
E1-7	0.5° S of warm-core	0.88	33.87	34.8	1.56	23.3	0.31
E1-8	1° S of warm-core	1.04	33.93	35.2	1.51	22.3	0.23
E2-1	2.5° E of warm-core	1.09	33.92				
E2-2	1.75° E of warm-core	1.27	33.99	31.2	1.46	20.1	0.44
E2-3	1° E of warm-core	1.71	33.96	26.2	1.51	21.5	0.49
E2-4	0.25° E of warm-core	1.62	33.97	29.0	1.56	22.5	0.33
E2-5	0.5° W of warm-core	1.60	33.96	29.7	1.60	22.7	0.44
E2-6	1.25° W of warm-core	1.60	33.98	29.1	1.49	22.4	0.42
E3-1	1.9° W of warm-core	1.69	34.04				
E3-2	0.73° W of warm-core	3.45	33.80	13.7	1.39	21.9	0.24
E3-3	Warm-core	4.70	33.77	4.4	1.34	20.2	0.18
E3-4	0.78° E of warm-core	4.76	33.77	3.5	1.34	19.5	0.18

ESSDD
8, 809–825, 2015

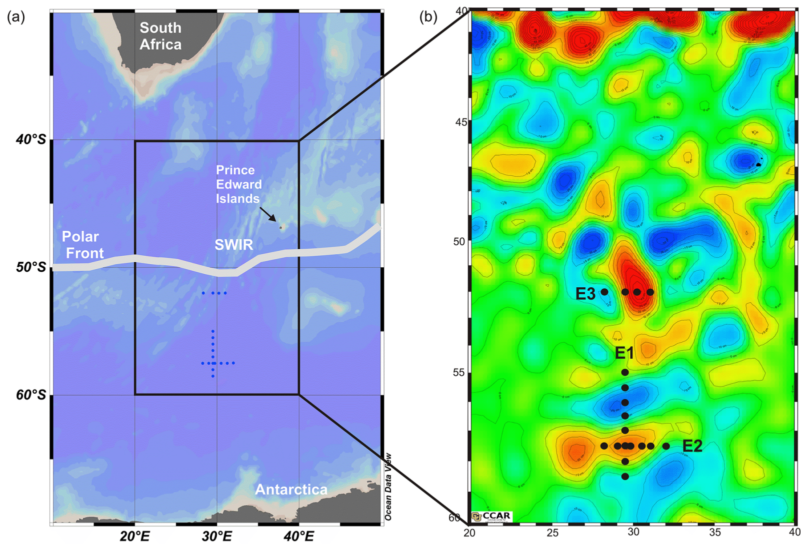

Figure 1. (a): Seafloor bathymetry in the southwestern Indian Ocean sector of the Southern Ocean, to indicate the position of the Southwest Indian Ridge (SWIR); shown in grey is the average position of the Polar Front (adapted from Dong et al., 2006); **(b)**: Superimposed upon a satellite altimetry map is the position of the transect lines, E1 to E3, situated between 52 to 58.5° S, south of the Prince Edward Island group; black dots indicate the location of CTD stations; red indicated positive SSH anomalies and blue indicate negative SSH anomalies

ESSDD
8, 809–825, 2015

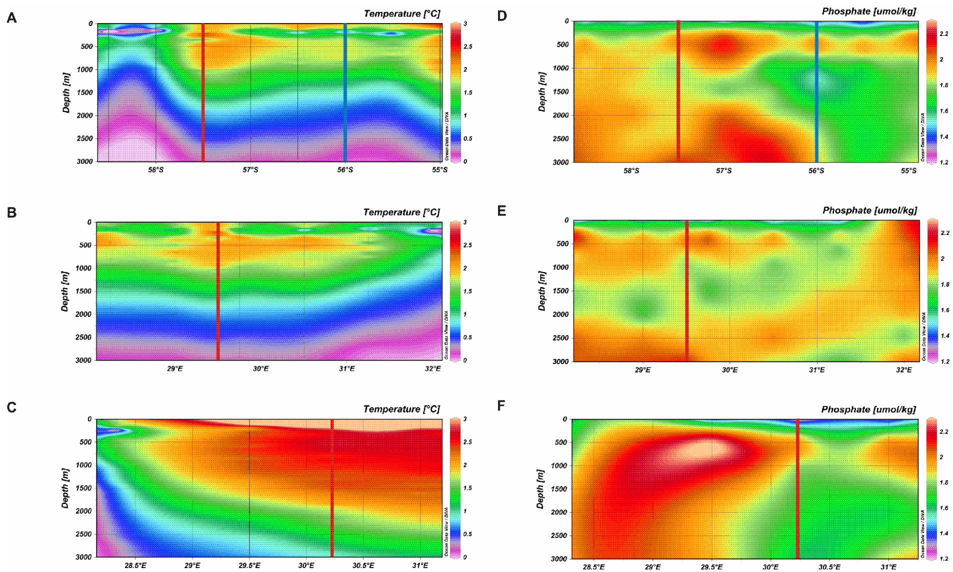

Figure 2. Temperature and dissolved phosphate profile data to a depth of 3000 m, for Transect E1 (**a** and **d**), Transect E2 (**b** and **e**) and Transect E3 (**c** and **f**). Vertical red lines (at 57.5° S in **a** and **d**, 29.5° E in **b** and **e**, and 30.25° E in **c** and **f**), indicate the approximate position of warm-core eddies (as described in Table 1), and vertical blue lines (56° S in **a** and **d**) similarly indicate the position of the cold-core eddy feature. The data available online (at http://doi.pangaea.de/10.1594/PANGAEA.848875) can be used to reproduce these Ocean Dataviewer (Schlitzer, R., Ocean Data View, odv.awi.de, 2015) plots, to shallower or deeper depths.

ESSDD
8, 809–825, 2015

In situ measurement of the biogeochemical properties

S. de Villiers et al

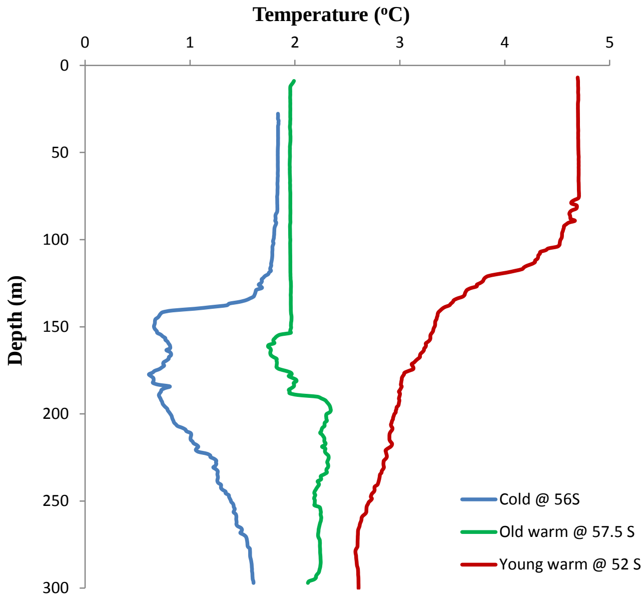

Figure 3. Upper 300 m water column temperature profiles, from CTD stations located at the approximate cores of the three main mesoscale features present along the transect lines: in blue the cold-core eddy (CTD station E1-3 in Table 1), in green the older warm-core eddy (E1-6) and in red the younger warm-core eddy (E3-3).

ESSDD
8, 809–825, 2015

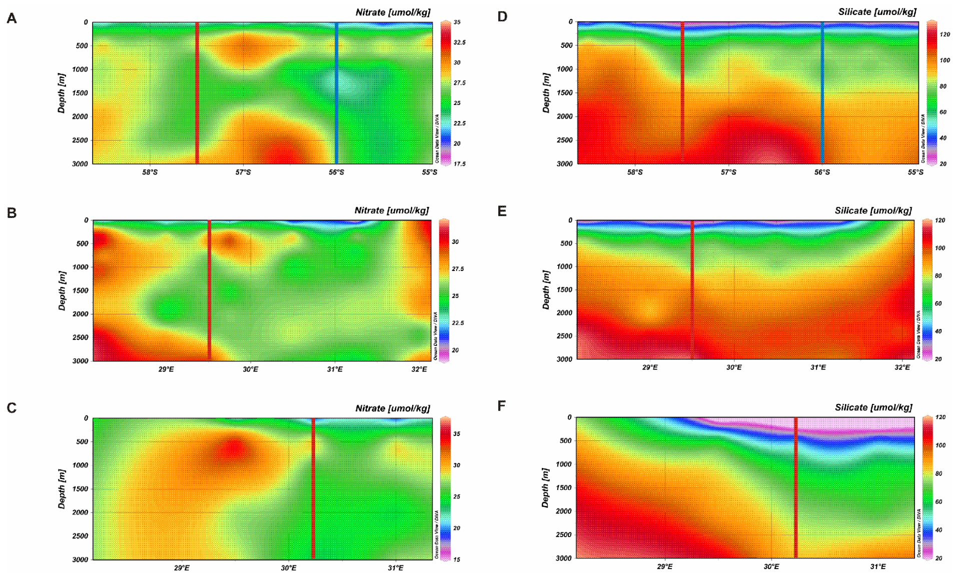

Figure 4. Dissolved nitrate and silicate profiles, plotted to a depth of 3000 m, for Transect E1 (**a** and **d**), Transect E2 (**b** and **e**), and Transect E3 (**c** and **f**). Vertical red and blue lines represent the eddy cores as described for Fig. 2. The data available online can be used to reproduce these Ocean Dataviewer plots, to shallower or deeper depths.

ESSDD
8, 809–825, 2015

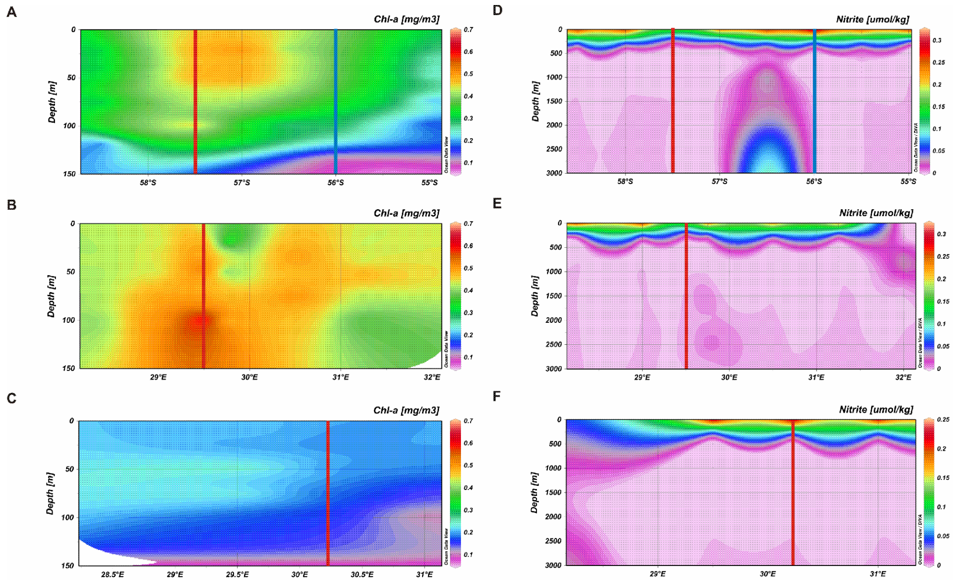

Figure 5. Chlorophyll *a* and dissolved seawater nitrite profiles, plotted to a depth of 150 m, for Transect E1 (**a** and **d**), Transect E2 (**b** and **e**), and Transect E3 (**c** and **f**). Vertical red and blue lines represent the eddy cores as described for Fig. 2. The data available online can be used to reproduce these Ocean Dataviewer plots, to shallower or deeper depths.

ESSDD
8, 809–825, 2015